Direct Measurements of Presynaptic Calcium and Calcium-Activated Potassium Currents Regulating Neurotransmitter Release at Cultured *Xenopus* Nerve–Muscle Synapses

Bruce Yazejian,[1] David A. DiGregorio,[1] Julio L. Vergara,[1] Robert E. Poage,[2] Stephen D. Meriney,[2] and Alan D. Grinnell[1]

[1]*Department of Physiology, Jerry Lewis Neuromuscular Research Center, University of California Los Angeles School of Medicine, Los Angeles, California 90095, and* [2]*Department of Neuroscience, University of Pittsburgh, Pittsburgh, Pennsylvania 15260*

The understanding of neurotransmitter release at vertebrate synapses has been hampered by the paucity of preparations in which presynaptic ionic currents and postsynaptic responses can be monitored directly. We used cultured embryonic *Xenopus* neuromuscular junctions and simultaneous pre- and postsynaptic patch-clamp current-recording procedures to identify the major presynaptic conductances underlying the initiation of neurotransmitter release. Step depolarizations and action potential waveforms elicited Na and K currents along with Ca and Ca-activated K (K_{Ca}) currents. The onset of K_{Ca} current preceded the peak of the action potential. The predominantly ω-CgTX GVIA-sensitive Ca current occurred primarily during the falling phase, but there was also significant Ca^{2+} entry during the rising phase of the action potential. The postsynaptic current began a mean of 0.7 msec after the time of maximum rate of rise of the Ca current. ω-CgTX also blocked K_{Ca} currents and transmitter release during an action potential, suggesting that Ca and K_{Ca} channels are colocalized at presynaptic active zones. In double-ramp voltage-clamp experiments, K_{Ca} channel activation is enhanced during the second ramp. The 1 msec time constant of decay of enhancement with increasing interpulse interval may reflect the time course of either the deactivation of K_{Ca} channels or the diffusion/removal of Ca^{2+} from sites of neurotransmitter release after an action potential.

Key word: neuromuscular junction; nerve terminal; calcium channel; charybdotoxin; conotoxin; synaptic delay

Neurotransmitter release from nerve terminals is triggered by the entry of Ca^{2+} through voltage-gated Ca channels (Katz, 1969; Augustine et al., 1987). Our understanding of the relationship between the presynaptic ionic currents and release is based largely on studies of the squid giant synapse (Katz and Miledi, 1967; Llinás et al., 1981; Charlton et al., 1982; Augustine et al., 1985a,b). Several critical questions remain, however, that one would like to address with equivalent biophysical rigor at a vertebrate synapse in which the presynaptic ionic currents and postsynaptic currents can be measured simultaneously and release can be resolved at the single quantum level. In this report we take advantage of a neuromuscular synapse preparation in which this can be done.

Among the important pending questions are the timing and delay between Ca^{2+} entry during an action potential and release, the roles of different Ca and Ca-activated K (K_{Ca}) channels in the release process, and the quantitative relationship between Ca^{2+} influx and release. In squid, it has been shown that Ca^{2+} enters principally during the repolarization phase of the action potential (Llinás et al., 1982). Physiological studies of various excitable secretory cells have shown that different types of Ca channels play a dominant role in triggering release in different terminals, and often multiple Ca channel types are present in any given terminal (Kerr and Yoshikami, 1984; Pfrieger et al., 1992, Luebke et al., 1993; Artalejo et al., 1994; Dunlap et al., 1994; Fu and Huang, 1994; Regehr and Mintz, 1994; Yawo and Chuhma, 1994; Mintz et al., 1995; Sivaramakrishnan and Laurent, 1995; Wheeler et al., 1996). In many nerve terminals, K_{Ca} channels are present, and in some cases they seem to be colocalized with Ca channels, potentially with important functional consequences (Augustine and Eckert, 1982; Lancaster and Nicoll, 1987; Lindgren and Moore, 1989; Roberts et al., 1990; Robitaille and Charlton, 1992; Robitaille et al., 1993; 1994; Blundon et al., 1995; Wheeler et al., 1996). Under different conditions and in different synapses, the relationship between external Ca^{2+} concentration or measured Ca^{2+} influx and release is a power function with an exponent ranging from 1 to 5 (Dodge and Rahamimoff, 1967; Katz and Miledi, 1970; Llinas et al., 1981; Cohen and Van der Kloot, 1985; Augustine and Charlton, 1986; Stanley, 1986; Augustine, 1990; Borst and Sakmann, 1996; Takahashi et al., 1996).
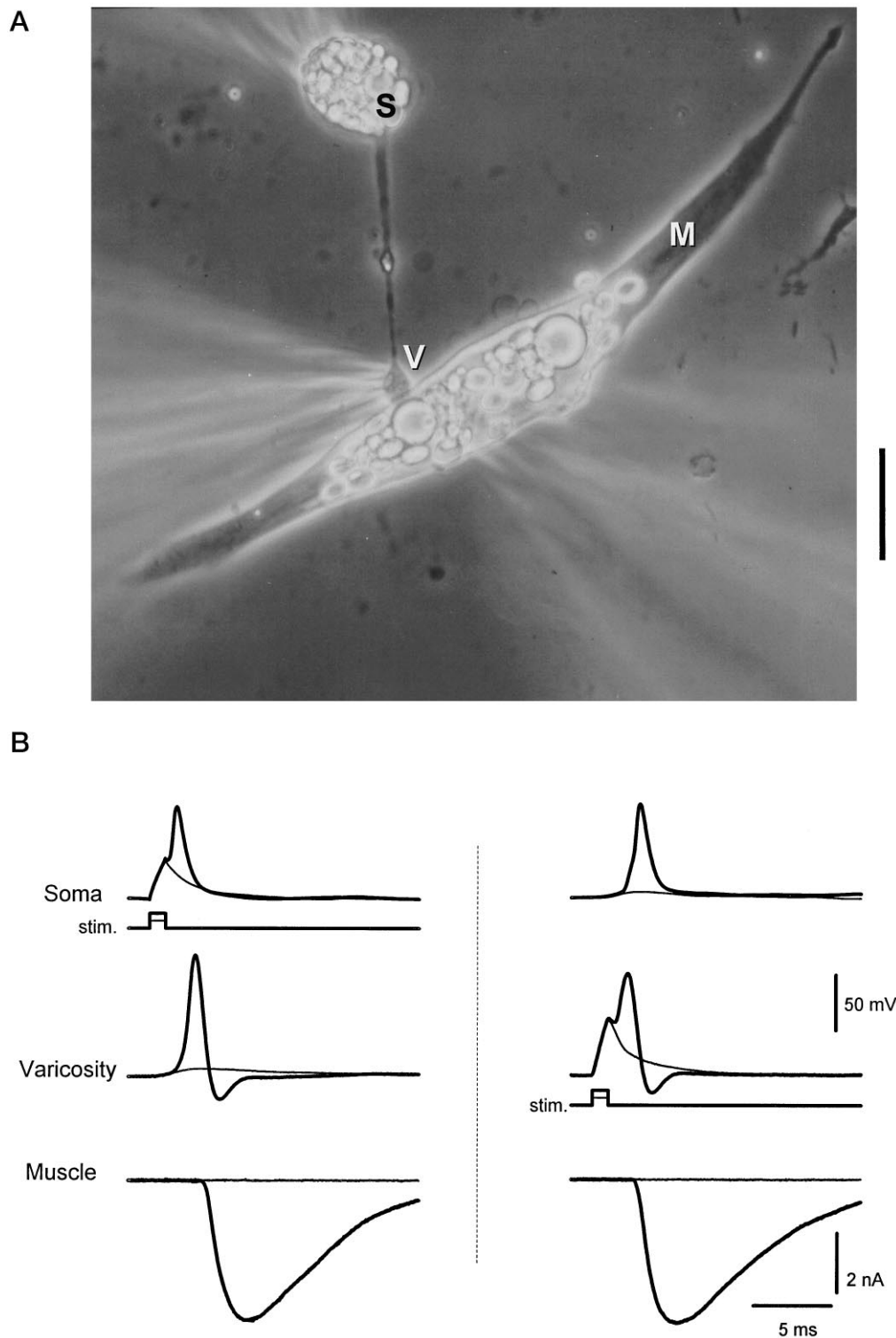
Intense interest in these problems has stimulated attempts to obtain answers in a number of vertebrate preparations (Lim et al., 1990; Stanley and Goping, 1991; Stanley, 1993; Yawo and Momiyama, 1993; Artalejo et al., 1994; Heidelberger et al., 1994; Borst et al., 1995; Sivaramakrishnan and Laurent, 1995; Borst and Sakmann, 1996; Takahashi et al., 1996). In this paper, we describe results from a novel preparation that offers the accessibility and degree of control of pre- and postsynaptic currents that are needed to obtain answers to many of these questions.

A

B

Figure 1. Triple patch-clamp recording from a synaptically coupled cell pair in culture. *A*, Phase-contrast photomicrograph of a representative preparation. Electrodes for patch recordings are placed on the neuronal soma (*S*), presynaptic neuronal varicosity (*V*), and postsynaptic muscle cell (*M*). Recordings were made in current clamp in the neuron at both locations and in voltage clamp in the muscle. Scale bar, 20 μm. *B, Left*, A subthreshold depolarization of the neuronal soma (*stim.*) evoked passive responses in the soma and varicosity and failed to evoke transmitter release (*thin traces*). Suprathreshold current injection evoked a somal action potential that propagated to the presynaptic varicosity and resulted in the release of transmitter, detected as an endplate current in the muscle cell (*thick traces*). *Right*, Direct stimulation of the presynaptic varicosity with a current step evoked an action potential that caused the release of transmitter (*thick traces*). The locally generated action potential back-propagated to the soma. Subthreshold depolarization of the varicosity did not evoke transmitter release (*thin traces*). Internal solution A was used for the soma and muscle recording; internal solution B was used for the varicosity recording. Resting potentials were the following: *Soma*, −65 mV; *Varicosity*, −69 mV. Similar results were seen in four other preparations.

Here we describe experiments using simultaneous pre- and postsynaptic voltage clamp in *Xenopus* nerve–muscle cocultures and characterize the ionic currents of the presynaptic varicosities. Previous work on this preparation measured Na currents (Kidokoro and Sand, 1989) and Ca currents (Hulsizer et al., 1991; Meriney et al., 1991) in varicosities. In this report, we emphasize the currents carried by the N-type Ca channels and K_{Ca} channels

that are functionally coactivated in presynaptic varicosities and coupled to transmitter release.

MATERIALS AND METHODS

Cell culture. Nerve–muscle cocultures were prepared on the basis of methods described previously (Spitzer and Lamborghini, 1976; Tabti and Poo, 1991). In brief, stage 20–22 *Xenopus laevis* embryos (Niewkoop and

Faber, 1967) were rinsed in sterile 10% normal frog Ringer's solution (NFR) (116 mM NaCl, 1 mM NaHCO$_3$, 2 mM KCl, 1.8 mM CaCl$_2$, 1 mM MgCl$_2$, 5 mM HEPES, 3 mM D-glucose, pH 7.3), and the spinal cord and associated myotomes were dissected away and allowed to dissociate in a Ca^{2+}- and Mg^{2+}-free Ringer's solution (125 mM NaCl, 2 mM KCl, 1.2 mM EDTA, and 5 mM Na-HEPES, pH 7.4) for 30–60 min. Disaggregated cells were then plated onto glass coverslips or plastic tissue-culture dishes and incubated at room temperature (22–24°C) for 24–48 hr in a medium composed of 49% NFR and 51% L-15 (Life Technologies, Gaithersburg, MD) supplemented with 3 mg/ml glutamine, 0.1 mg/ml insulin, 0.7 mg/ml sodium selenite, 0.6 mg/ml transferrin, 1 mg/ml sodium pyruvate, and 35 ng/ml brain-derived neurotrophic factor [kindly provided by Amgen (Thousand Oaks, CA) and Regeneron (Tarrytown, NY)]. In as little as 12 hr, spinal neurons extended neurites, occasionally elaborating varicose regions on the substrate and in contact with spindle-shaped muscle cells (Kidokoro and Yeh, 1982; Takahashi et al., 1987; Evers et al., 1989; Tabti and Poo, 1994). In 1 and 2 d cultures, the presynaptic contact often takes the form of a varicosity sufficiently large to be accessed with patch electrodes, allowing one to correlate presynaptic electrophysiological events with transmitter release. These synapses exhibit properties–both physiological and morphological–that appear to parallel closely those of their developing counterparts *in vivo* (Kullberg et al., 1977). Within hours of contact, they resemble mature cholinergic synapses in many respects. They exhibit spontaneous release, high quantal content-evoked release, membrane thickenings, clouds of vesicles, and postsynaptic aggregation of ACh receptors (Anderson et al., 1977; Weldon and Cohen, 1979; Cohen and Weldon, 1980; Kidokoro et al., 1980; Kidokoro and Yeh, 1982; Brehm et al., 1984; Takahashi et al., 1987; Buchanan et al., 1989; Evers et al., 1989).

Electrophysiology. Traditional whole-cell recording techniques were used to record voltages and currents from neuronal somata and muscle cells. Patch electrodes of 2–4 MΩ were filled with a quasi-internal solution (internal solution A) of the following composition (in mM): 116 KCl, 1 NaCl, 1 MgCl$_2$, 10 EGTA, 5 HEPES, pH 7.3. Because the Ca current at presynaptic varicosities is labile, we adopted a modification of the perforated patch recording configuration (Horn and Marty, 1988) for use in recording at the varicosity. For current clamp and in experiments designed to measure both K and Ca currents, the presynaptic pipette was filled with internal solution B (in mM): 52 K$_2$SO$_4$, 38 KCl, 1 EGTA, and 5 HEPES, pH 7.3, plus 900 μg/ml amphotericin B (Rae et al., 1991). Except where noted, for experiments designed to isolate Ca currents, the pipette was filled with internal solution C (in mM): 52 CsMeSO$_4$, 38 CsCl, 1 EGTA, 1 3,4 diaminopyridine (3,4 DAP), 50 D-glucose, and 5 HEPES, pH 7.3, plus 900 μg/ml amphotericin B. Similarly, the bath solution for all experiments was NFR, unless noted otherwise. Voltage-clamp depolarization waveforms (pCLAMP version 6.02, Axon Instruments, Foster City, CA) were followed by two identical hyperpolarizing waveforms of one-half or four of one-quarter amplitude for linear leak and capacitive current subtraction (P/−2 subtraction method was used for all voltage-clamp experiments except those of Fig. 5D, in which P/−4 was used). We selected for use varicosities yielding records with fast tail currents, indicating good spatial control of voltage at sites of current flow, and accepted perforated patch recordings with series resistances under 20 MΩ. In all experiments, the holding potentials were −70 mV (varicosity) and −80 mV (muscle cell). Currents and voltages were recorded with patch-clamp amplifiers (Axopatch 1B, 200, 200A; Axon Instruments), filtered with a 4-pole Bessel filter at 5–10 kHz digitized at 111–167 kHz, and stored on a PC-based microcomputer for analysis. Action potentials were recorded in somas using the Axopatch 1B and in the varicosities using the Axopatch 200A (I-clamp, normal setting). Off-line digital Gaussian filtering was performed at 10–20 kHz for the creation of the figures. In some cases, up to 100 μsec of the capacitance current artifacts were blanked.

RESULTS

Patch recording configurations

Figure 1*A* illustrates a representative preparation, consisting of a motoneuron soma (*S*) and its neurite, ending in a synaptic varicosity (*V*) on a muscle cell (*M*). Sometimes the varicosities were simply enlargements of a neurite that made contact with a muscle cell *en passant*. In the case illustrated in Figure 1, the neuron soma, its varicosity, and the muscle cell were simultaneously patch-clamped—the varicosity with the perforated patch method
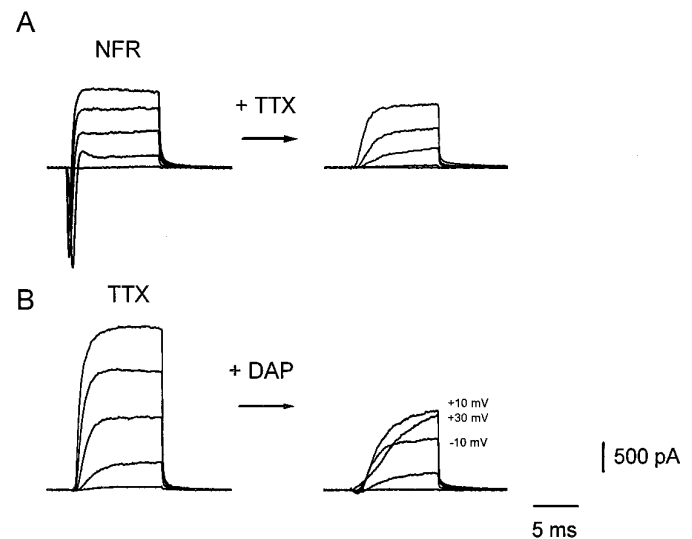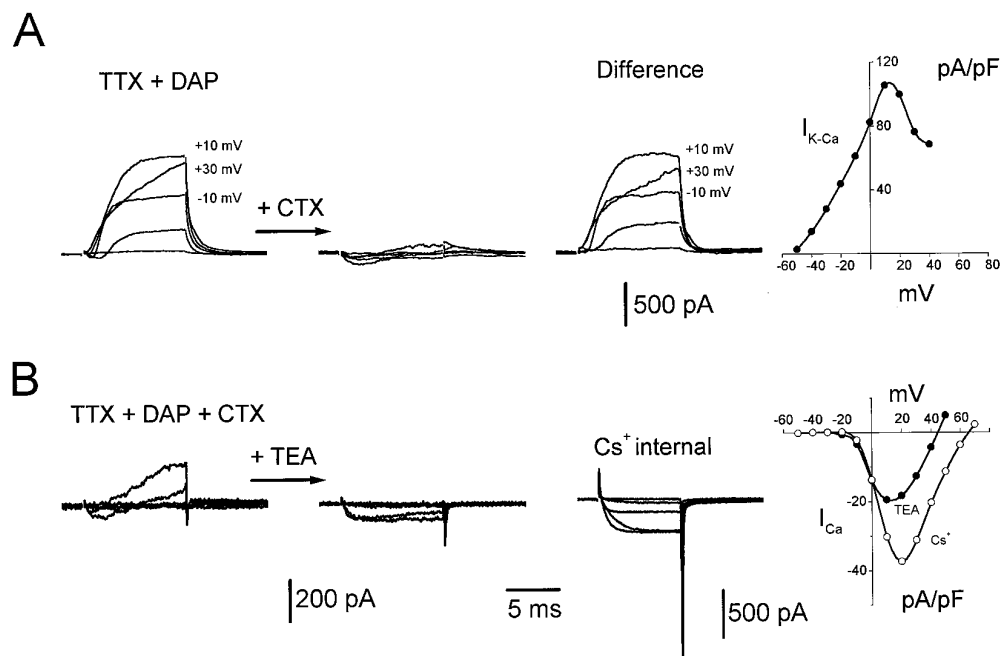

Figure 2. The major presynaptic ionic currents. Representative currents evoked by depolarizing steps of voltage from a holding potential of −70 mV to −30, −10, +10, +30, and +50 mV are shown. *A*, Presynaptic currents evoked before (*left*) and after (*right*) application of 300 nM tetrodotoxin (*TTX*). Similar results were seen in six other preparations. *B*, *Left*, Presynaptic currents in TTX; *right*, after addition of 1 mM 3,4 diaminopyridine (*DAP*). Note that at higher voltages (see values given next to the traces) the current does not increase linearly with potential. *A* and *B* were taken from different varicosities. Internal solution B was used. Similar results were obtained in four other preparations.

(Horn and Marty, 1988) to avoid washout of cytoplasmic contents. This triple-patch configuration was used to demonstrate that an action potential could be generated in either the soma or the varicosity, eliciting postsynaptic currents that were equivalent in magnitude and time course (Fig. 1*B*).

Severing the neurite between the varicosity and the soma did not prevent either the generation of an action potential in the varicosity or the release of transmitter, and it had no significant effect on the action potential waveform, although the undershoot was slightly reduced (data not shown). Because our primary interest was in the correlation between presynaptic ionic currents and transmitter release, in subsequent experiments we restricted our measurements to the varicosity and the muscle cell. Unless specified otherwise, we ensured that the varicosity was forming a functional synapse by simultaneously monitoring transmitter release from the postsynaptic muscle cell. This was true even for those experiments in which only the presynaptic currents are shown (e.g., Figs. 2, 3). EPSCs, recorded under voltage-clamp conditions, were used to assess neurotransmitter release because of their greater accuracy (Katz and Miledi, 1979), and to prevent muscle contraction.

Presynaptic currents and transmitter release with step depolarizations

To measure the electrophysiological properties of the presynaptic membranes, we voltage-clamped the varicosity and dissected ionic currents by applying specific channel blocking agents in turn (Figs. 2, 3). In NFR, depolarizing voltage steps evoked large, transient inward currents followed by delayed outward currents (Fig. 2*A*, *left*) reminiscent of the Na and K currents classically described in squid axon (Hodgkin and Huxley, 1952). The inward current was blocked by tetrodotoxin (TTX) (Fig. 2*A*, *right*). It should be noted that this current was too large to be maintained under adequate

Figure 3. Isolation of the minority presynaptic ionic currents. Representative currents evoked by depolarizing steps of voltage from a holding potential of −70 mV to −50, −30, −10, +10, and +30 mV are shown. *A*, Presynaptic currents in *TTX + DAP* (*left set of traces*) and after (*middle set*) the addition of 100 nM charybdotoxin (*CTX*). The right set of traces was obtained by subtraction of the middle set of traces from the left set. Voltage values given next to the current traces indicate that the CTX-sensitive outward current was depressed at higher voltages. *Right*, *I–V* plot generated from the difference traces for values 8 msec into the step. Currents were normalized to the cell capacitance. Similar results were seen in 10 other experiments. *B*, *Left*, Presynaptic currents in *TTX + DAP + CTX*. *Middle set of traces*, After addition of 20 mM tetraethylammonium Cl⁻ (*TEA*). The right set of traces was obtained from a different cell after replacement of the internal K⁺ with Cs⁺ (*Cs⁺ internal*) and an increase of the external Ca²⁺ to 10 mM. *Right*, Plots of maximum Ca current versus voltage obtained from the middle set of traces (*TEA, filled symbols*) and the right set of traces (*Cs⁺, open symbols*). Currents were normalized to the cell capacitance. Similar results were seen in three other preparations (*TEA*) and in 12 other preparations (*Cs⁺ internal*). *A* and *B* were taken from different varicosities. Internal solution B was used, except for the panel labeled *Cs⁺ internal* where internal solution C was used.

voltage clamp, given the resistance in series with the electrode in the perforated-patch method (10–15 MΩ).

As is illustrated in Figure 2*B* in an experiment with another synapse, in the presence of TTX much of the outward current was blocked by the subsequent application of 3,4 DAP. Like the TTX-sensitive currents (Fig. 2*A*), these outward currents were often too large to be adequately voltage-clamped with the perforated-patch method.

The residual currents obtained after the addition of DAP and TTX (Fig. 2*B*, *right*) displayed two interesting features. First, an inward current preceded an outward current, and second, at large depolarizations the inward current was not visible and the outward current began to decline in magnitude. These features suggested the presence of an early inward Ca current activating a delayed outward K_{Ca} current (Marty, 1981; Blatz and Magleby, 1984). Figure 3*A* (first two sets of traces) demonstrates that a large fraction of the outward current was blocked by charybdotoxin (CTX), a blocker of the high conductance K_{Ca} channel (Miller et al., 1985). Similar effects were observed with iberiotoxin, another blocker of the large K_{Ca} channel (Candia et al., 1992) (data not shown). The observation that the block of the outward current by CTX was incomplete (Fig. 3*A*, second set of traces) may be explained by the fact that the CTX block of K_{Ca} channels is reversed by large depolarizations (MacKinnon and Miller, 1988) or that higher concentrations of CTX are needed. The bell shape of the *I–V* plot of the CTX-sensitive current (Fig. 3*A*, *right*; obtained from the *Difference* records) supports the conclusion that this is a K_{Ca} current, and it will hereafter be termed I_{K-Ca}.

The residual outward current that was insensitive to block by either DAP or CTX (Fig. 3*A*, middle set of traces; 3*B*, left set of traces) was blocked by tetraethylammonium chloride (TEA), revealing a sustained inward current (Fig. 3*B*, second sets of traces). This inward current was blocked completely by 100 μM CdCl₂ (data not shown) and will hereafter be termed I_{Ca}. This I_{Ca} is characterized by the *I–V* plot at the right of Figure 3*B* (*filled symbols*). It should be noted that the peak of this *I–V* (at approximately +10 mV) is coincident with the peak of the I_{K-Ca} *I–V* (Fig. 3*A*, *right*), further supporting the assertion that the CTX-sensitive current (Fig. 3*A*, *Difference* records) is Ca²⁺-activated. Although this combination of pharmacological agents was relatively effective at isolating Ca currents, the inward current often was still contaminated by a small residual outward current if the internal presynaptic electrode contained K⁺. Moreover, because extracellular TEA blocks postsynaptic ACh receptors (Katz and Miledi, 1979), its use was contraindicated in studies designed to investigate the relationship between presynaptic Ca currents and transmitter release. Both problems could be circumvented by replacing the K⁺ in the recording pipette with Cs⁺. With this electrode solution, and the use of 10 mM Ca²⁺ in combination with TTX and DAP in the bathing solution, almost all of the outward current could be suppressed, allowing near-complete isolation of the presynaptic Ca current (Fig. 3*B*, *third panel*, labeled *Cs⁺ internal*). Close inspection of the traces of Figure 3*B* (especially the *third panel*) reveals that at the onset of the voltage steps there were rapid, transient outward currents that could not be subtracted with the P/−2 pulse protocol (see Materials and Methods). These were seen even for small depolarizations and thus were not
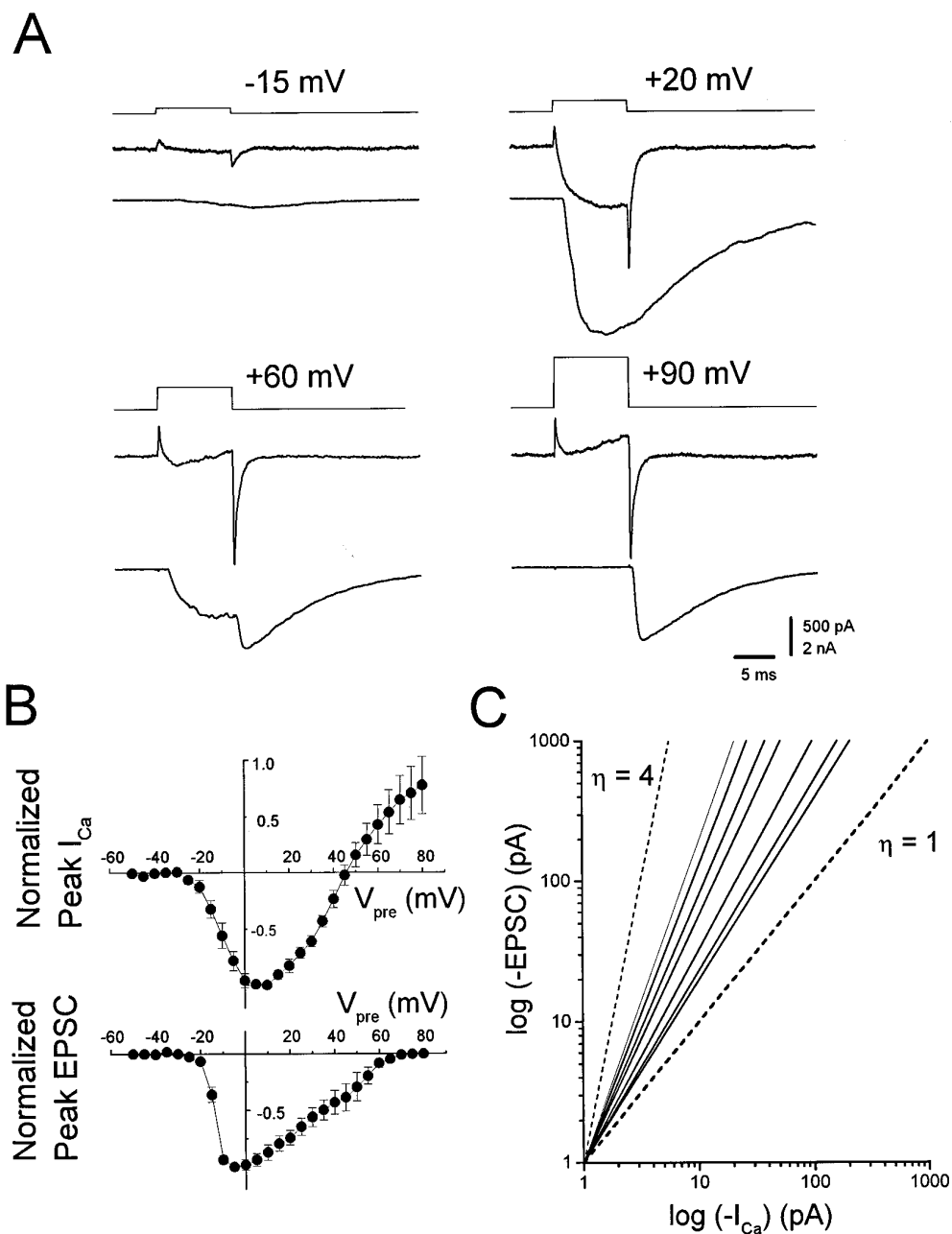
Figure 4. Current–voltage relationships of presynaptic Ca current and EPSCs. *A*, Representative experimental results showing depolarizing steps of voltage from a holding potential of −70 mV to specified voltages (*top traces*) evoking Ca currents (*middle traces*) linked to transmitter release transmitter release (EPSCs, *bottom traces*). A depolarizing step to +20 mV evoked a larger Ca current and a correspondingly larger EPSP than a step to −15 mV. At +60 mV the Ca current was suppressed during the step, resulting in less release. An off-response was apparent that corresponded to the large Ca tail current. At +90 mV, the Ca current and release were suppressed, but a large off-response was seen in response to the tail current. *B*, Current–voltage plots for seven synapses normalized to the maximum current value seen for each synapse plotted as a function of the presynaptic potential. *Top graph*, Peak presynaptic Ca current; *bottom graph*, peak postsynaptic current. Error bars in this and all figures represent SD. Internal solution C was used for all experiments. The external solution was NFR containing 300 nM TTX and 1 mM DAP. *C*, Double log plots of the presynaptic current measured at 9 msec into the step versus peak postsynaptic current. The *solid lines* are least-squares fits of the data from the same seven synapses illustrated in Figure 4*B*, using only the currents activated between −35 and −5 mV (see text). The range of slopes obtained for these cells was 1.30 to 2.29. For comparison, first-power ($\eta = 1$) and fourth-power ($\eta = 4$) functions have been plotted as *dashed lines*.

artifacts caused by saturation of the amplifier by the capacitive transients. These may represent gating currents of the various voltage-gated channels in the varicosity.

The isolation of the presynaptic I_{Ca} by using internal Cs^+ and external TTX and DAP allowed us to correlate the Ca^{2+} entry into varicosities with transmitter release. Figure 4*A* shows a family of presynaptic currents and corresponding EPSCs obtained over a range of presynaptic voltage steps in a synapse bathed in normal extracellular Ca^{2+} (1.8 mM). As expected, with depolarizations to membrane potentials approaching the Ca^{2+} reversal potential, the Ca current and the EPSC during the voltage step were suppressed. With these larger depolarizations, an increasing percentage of the EPSC arose from the Ca tail current at the end of voltage step (for example, see +60 and +90 mV). Peak presynaptic I_{Ca} ranged from 95 to 934 pA, whereas the peak EPSC ranged from 1 to 15 nA. Figure 4*B* illustrates the mean current-to-voltage relationships of

both the presynaptic varicosity (*top panel*) and the postsynaptic muscle cell (*bottom panel*) when measured simultaneously. In this correlation of the presynaptic Ca current with neurotransmitter release, we chose only those synapses in which the peak postsynaptic current was <5 nA. This was done to minimize the voltage error resulting from resistance in series with our pipettes. Note that the low-voltage arm of the Ca current *I–V* relationship is shallower than the corresponding arm of the EPSC *I–V*, consistent with a power-law relationship. Curiously, the peak of the EPSC *I–V* occurs at lower voltages than does the Ca current *I–V*, which is inconsistent with a simple power law and may imply saturation of the synaptic transfer function. The fact that the presynaptic current reversed polarity before the postsynaptic response decrements to zero is a reflection of contamination of the Ca current with an outward current. Finally, the asymmetry in the EPSC *I–V* implicates a possible asymmetry in the release process.
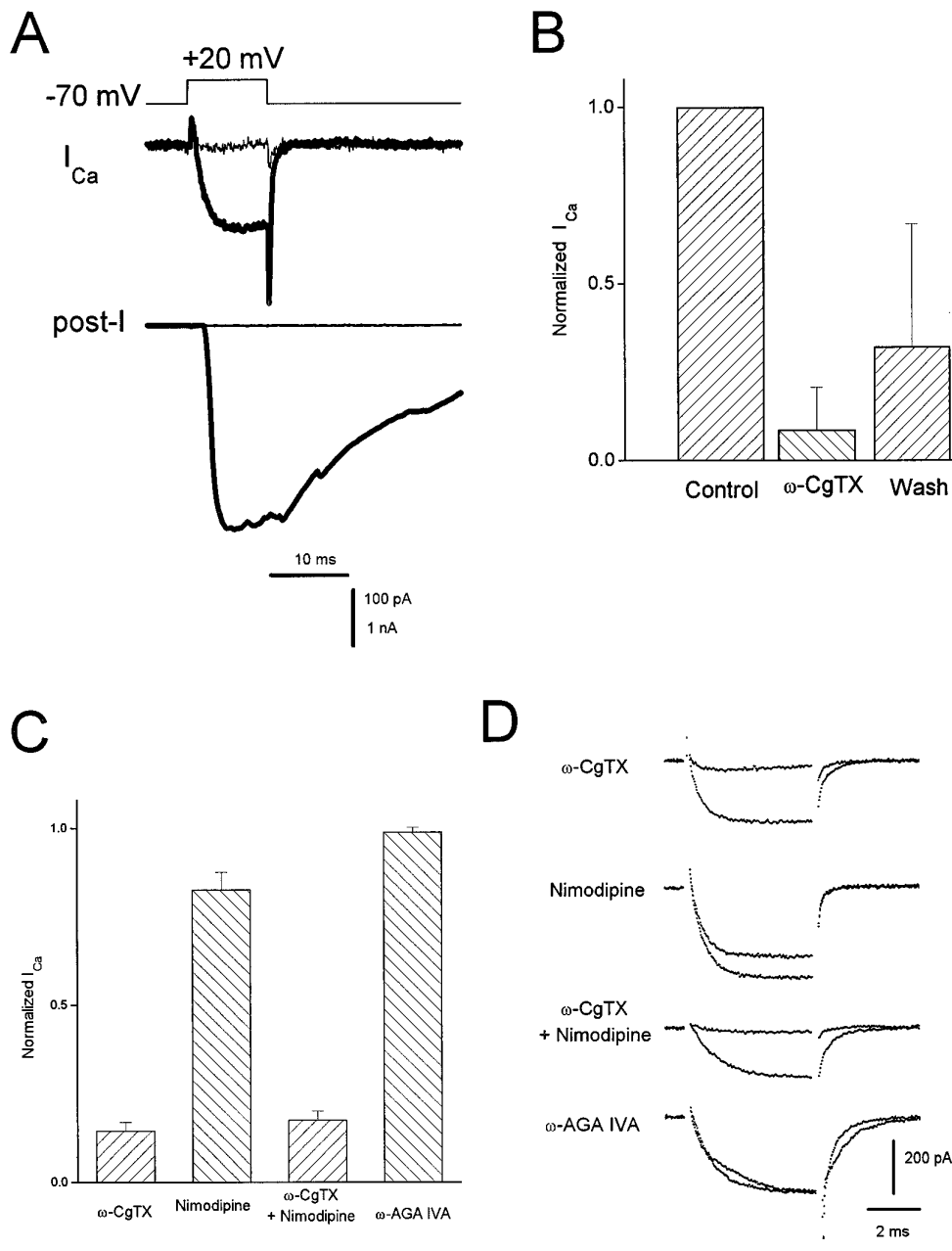
Figure 5. Pharmacology of presynaptic Ca currents and transmitter release. *A, Thick traces,* A depolarizing step of voltage evoked an inward Ca current (I_{Ca}) correlated with a large EPSC (*post-I*). After application of 1 μM ω-conotoxin GVIA (*ω-CgTX*), all transmitter release was eliminated, as was most of the Ca current (*thin traces*). Internal solution C was used in the presynaptic pipette. The external solution was NFR containing 300 nM TTX and 1 mM DAP. *B,* Bar graph showing the degree and reversibility of block of presynaptic Ca current by 1 μM ω-CgTX ($n = 6$). In all cases, block of transmitter release was complete, with little or no recovery after wash. *C,* Bar chart indicating the percentage of varicosity Ca current remaining after application of 2 μM ω-CgTX ($n = 8$), 2 μM nimodipine ($n = 3$), ω-CgTX plus nimodipine ($n = 4$), and 500 nM ω-AGA IVA ($n = 5$). In these studies, the Ca current was isolated using a combination of 1 μM TTX, 5 mM DAP, and 20 mM TEA in a 10 mM $CaCl_2$ bath solution and using internal solution of the following composition (in mM): 68 $CsMeSO_4$, 50 CsCl, 8 $MgCl_2$, 10 HEPES, pH 7.4. Currents were evoked by steps to +20 mV from a holding potential of −80 mV. *D,* Current traces (average of four) associated with treatments indicated by the *bars* in *C,* taken from representative experiments, showing currents before and after drug addition.

In Figure 4*C* we illustrate the quantitative relationship between the presynaptic Ca current and peak postsynaptic response for the same junctions from which we plotted the *I–V* values of Figure 4*B*. To determine the maximum power-law relationship, we chose the first few voltages (−35 mV to −5 mV) in which Ca^{2+} entry produced a postsynaptic response. At larger depolarizations outward current contamination made measurements of the Ca current unreliable. The slopes of the linear regression fits of these data yielded a mean value of 1.76 ± 0.36 (SD, $n = 7$), with a range of 1.30 to 2.29.

Pharmacology of Ca currents and transmitter release

Pharmacological tests showed that I_{Ca} in the varicosities was carried through more than one type of channel, only one of which seemed capable of mediating evoked transmitter release. The N-type Ca channel blocker ω-CgTX (1 μM) (Kerr and Yoshikami, 1984) reduced the varicosity I_{Ca} to ~8.6 ± 12% ($n = 6$) of the original value and blocked all neurotransmitter release ($n = 20$) (Fig. 5*A*). The I_{Ca} block was partially reversible. On average, washout of the toxin restored I_{Ca} within minutes to an average 32 ± 35% of control values ($n = 6$) (Fig. 5*B*). There was never full recovery of I_{Ca}, however, with little or no recovery of transmitter release. This suggests that there may be at least two types of ω-CgTX-sensitive Ca channels in these preparations: one that is blocked irreversibly and the other that is blocked reversibly (Jones and Marks, 1989; Plummer et al., 1989).

In a parallel series of experiments, the Ca current was completely isolated when a combination of internal Cs^+ and extracellular TEA with 10 mM $CaCl_2$ was used. For these experiments we did not simultaneously monitor neurotransmitter release, but endeavored to choose junctions where we saw muscles twitching (spontaneously or after stimulation). In this preparation, uninnervated muscle cells fail to contract. In these experiments, the

Figure 6. Use of the action potential waveform to study dynamics of presynaptic currents associated with transmitter release. *A*, In NFR, an action potential elicited in a presynaptic varicosity (*pre-V, left*) evoked transmitter release (*post-I*). *Right*, At the same synapse, a voltage-clamp action potential waveform (*VCAP*) generated by digitizing the evoked action potential (from the *left panel*) was used as the voltage command (*stim-V*). This elicited large early inward and delayed outward presynaptic currents (*pre-I*) evoking similar transmitter release as was seen in the left panel. Internal solution B was used. Similar results were seen at nine other synapses. *B*, At another synapse, use of a *VCAP* waveform, obtained by digitizing an action potential at another synapse, in the presence of TTX and DAP (*left*) reveals a smaller early outward Ca-activated K current followed by inward Ca current and evokes transmitter release. Subsequent addition of charybdotoxin (*CTX, right*) blocked the outward Ca-activated K current unmasking the transient presynaptic Ca current that evoked transmitter release. Internal solution B was used. Similar results were seen at 12 other synapses. *C*, More complete isolation of Ca current, achieved by using internal Cs^+ in place of K^+ (internal solution C), revealed a smaller early component of Ca current preceding the peak of the VCAP waveform followed by a larger component during the falling phase of the waveform. The Ca current terminated during the undershoot of the VCAP waveform. Bath solution was NFR + TTX + DAP. Similar results were seen at seven other synapses.
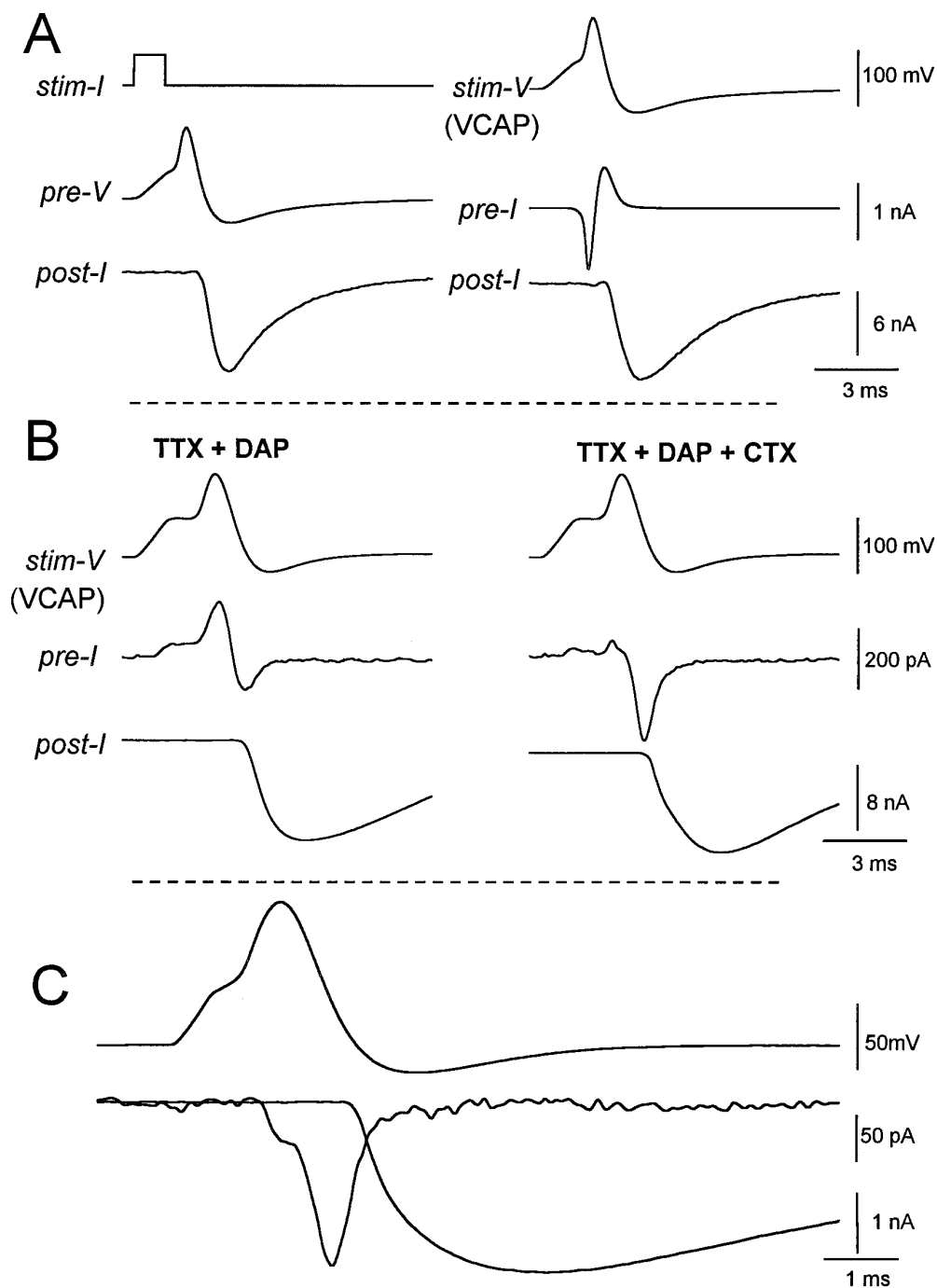
varicosity Ca current was reduced to 14.3 ± 2.5% by ω-CgTX (*n* = 8) and to 82.5 ± 5.1% by 2 μM dihydropyridine nimodipine (*n* = 3), but was insensitive to 500 nM ω-agatoxin IVA (*n* = 4), which blocks P-type channels (Mintz et al., 1992) (Fig. 5*C*). The block by ω-CgTX and nimodipine applied together was essentially the same as the block by ω-CgTX alone (Fig. 5*C*). This suggests that both drugs are working on the same Ca channels. Figure 5*D* shows representative experimental results from those pooled in Figure 5*C*. The nature of the remaining 15–17% of I_{Ca} not blockable by ω-CgTX or nimodipine is not known, but it is probably not attributable to T-type channels, which are activated with small depolarizations and exist in the soma (Barish, 1991); we saw no low voltage-activated component to I_{Ca}, and the ω-CgTX-

resistant I_{Ca} was insensitive to a decrease in the holding potential to −40 mV.

Presynaptic currents and transmitter release with action potential waveforms

One of the advantages of this coculture preparation is that it permits study of the activation kinetics of the presynaptic ionic currents underlying neurotransmitter release under physiological conditions of activation. We recorded action potentials elicited in varicosities (Fig. 6*A, left*) and then used the action potential waveforms as command voltages for varicosities in voltage-clamp experiments (Llinás et al., 1982; Yazejian et al., 1995; Borst and Sakmann, 1996). The EPSC occurred during the falling phase of

the action potentials (Fig. 6*A*, *left*) and during the downward stroke of the voltage-clamped action potential (VCAP) waveforms (Fig. 6*A*, *right*). The magnitude and delay of the evoked EPSCs were similar in both current-clamp and voltage-clamp conditions.

To study further the specific ionic currents underlying release, we blocked the major Na and K conductances in other varicosities with TTX and DAP. Under these conditions, the VCAP waveforms evoked biphasic ionic currents (linear currents were subtracted by the P/−2 method; see Materials and Methods) consisting of an early outward component correlated with the depolarizing phase of the voltage, followed by an inward current associated with the repolarizing phase (Fig. 6*B*, *left*). Each of these current components was much smaller than the Na current observed before block with TTX. Interestingly, CTX eliminated most of the early outward current, suggesting that this current is carried through K_{Ca} channels, and unmasked a prominent Ca current that preceded transmitter release (Fig. 6*B*, *right*).

After K^+ was replaced with Cs^+ in the presynaptic pipette, the time course of the isolated Ca current during a VCAP stimulation then could be compared with the release of transmitter and with the action potential (Fig. 6*C*). Interestingly, most of the Ca current occurred during the downstroke of the action potential; however, the inflection in the Ca current, which coincides with the peak of the action potential (Fig. 6*C*), reveals that significant Ca^{2+} entry can also occur during the upstroke of the action potential. This early Ca current may enable the activation of the prominent I_{K-Ca} seen in Figure 6*B*.
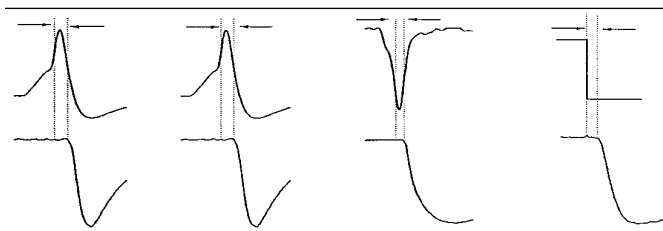
Synaptic delay

This preparation and the use of the VCAP waveform has allowed direct comparison of the timing of Ca^{2+} entry during an action potential with transmitter release. For comparison with studies in other preparations, we have also measured the characteristic delays from the time of maximum rate of rise of the action potential and from the termination of a depolarizing step to the onset of transmitter release (Table 1).

Evidence for coactivation of presynaptic Ca and K_{Ca} channels during an action potential

In mature neuromuscular junctions there is evidence for structural colocalization of N-type Ca channels and K_{Ca} channels (Robitaille and Charlton, 1992; Robitaille et al., 1993). A tight functional colocalization of dihydropyridine-sensitive (L-type) Ca channels and K_{Ca} channels has been demonstrated in amphibian hair cells (Roberts et al., 1990). To determine whether in our preparation there is this type of coactivation of N-type Ca channels and K_{Ca} channels during an action potential leading to transmitter release, we explored the effects of ω-CgTX on the activation of K_{Ca} channels. We used VCAP waveforms to elicit Ca and K_{Ca} currents mimicking those occurring during a physiological action potential. ω-CgTX blocked significantly both the inward Ca current and the outward K_{Ca} current, and eliminated transmitter release (Fig. 7*Ab*). Hence, K_{Ca} channels and neurotransmitter release are coactivated during an action potential by Ca current through N-type Ca channels. Interestingly, after washout of ω-CgTX, the K_{Ca} current component recovered within 20 sec, whereas the EPSC and the net inward current showed slower, incomplete recovery (Fig. 7*A*, *c* and *d*). The rapid recovery of the K_{Ca} current before full recovery of I_{Ca} and transmitter release suggests that the K_{Ca} channels display a higher affinity for Ca^{2+} ions, a closer proximity to the Ca channels, or different cooper-

Table 1. Synaptic delays measured with respect to different presynaptic parameters

A. AP $(dV/dt)_{max}$	B. VCAP $(dV/dt)_{max}$	C. VCAP $(dI_{Ca}/dt)_{max}$	D. VC step $(step)_{off}$
1.34 ± 0.22 msec	1.50 ± 0.14 msec	0.70 ± 0.11 msec	0.63 ± 0.12 msec
(n = 8)	(n = 9)	(n = 9)	(n = 7)

Synaptic delays were measured between each of the following and the onset of the postsynaptic response: A, the maximum rate of rise of the action potential in a current-clamp experiment (as in Figure 1*B*, *right panel*); B, the maximum rate of rise of voltage in a VCAP experiment performed in NFR (as in Figure 6*A*, *right*); C, the maximum rate of increase of the presynaptic Ca current in a VCAP experiment performed with internal solution C and with TTX and DAP in the bath (as in Figure 6*C*). D, The moment of repolarization after a voltage step to near E_{Ca} with internal solution C and TTX and DAP in the bath (as in Figure 4*A*, +90 mV).

ativity among Ca^{2+} ions for their activation than does the release mechanism. Nevertheless, these data demonstrate that Ca^{2+} entry under physiological conditions during an action potential can coactivate K_{Ca} channels and the release of neurotransmitter.

Because K_{Ca} channels respond to Ca^{2+} during an action potential, we used their activation as an assay of the decay of intracellular $[Ca^{2+}]$ after an action potential. We used a double-pulse paradigm with identical ramp waveforms and varied the interpulse interval. Figure 7*B* (*left*) shows that the early K_{Ca} current elicited during the rising phase of the first voltage ramp was greatly potentiated in the second ramp when the latter was delivered with an interpulse interval of under 4 msec. Increasing the interpulse interval led to decreased potentiation. We have shown previously with VCAP waveforms (Fig. 6*C*) that Ca^{2+} entry occurred primarily during the repolarization phase of the action potential. If one assumes that a similar time course of Ca^{2+} entry occurred with the ramp waveform, then it is conceivable that the potentiation of the K_{Ca} current in the second pulse of Figure 7*B* reflects the sensitivity of the K_{Ca} channel as a Ca^{2+} concentration sensor. The magnitude of the K_{Ca} current in response to the second ramp pulse is plotted against the interval between pulses in the right panel of Figure 7*B*. The decay time constant (τ) of the potentiation was ~1 msec and may represent the time course of deactivation of K_{Ca} channels or reflect the persistence of Ca^{2+} in the vicinity of K_{Ca} channels.

DISCUSSION

We describe here a novel use of a cultured *Xenopus* neuromuscular junction preparation. Presynaptic varicosities and postsynaptic muscle cells were patch-clamped to detect simultaneously the magnitude and time course of their respective ionic currents during synaptic transmission. After the major conductances responsible for the excitable properties of the presynaptic varicosity (Na and K_V) are blocked, the smaller residual conductances (Ca and K_{Ca}), which are potentially more interesting because of their
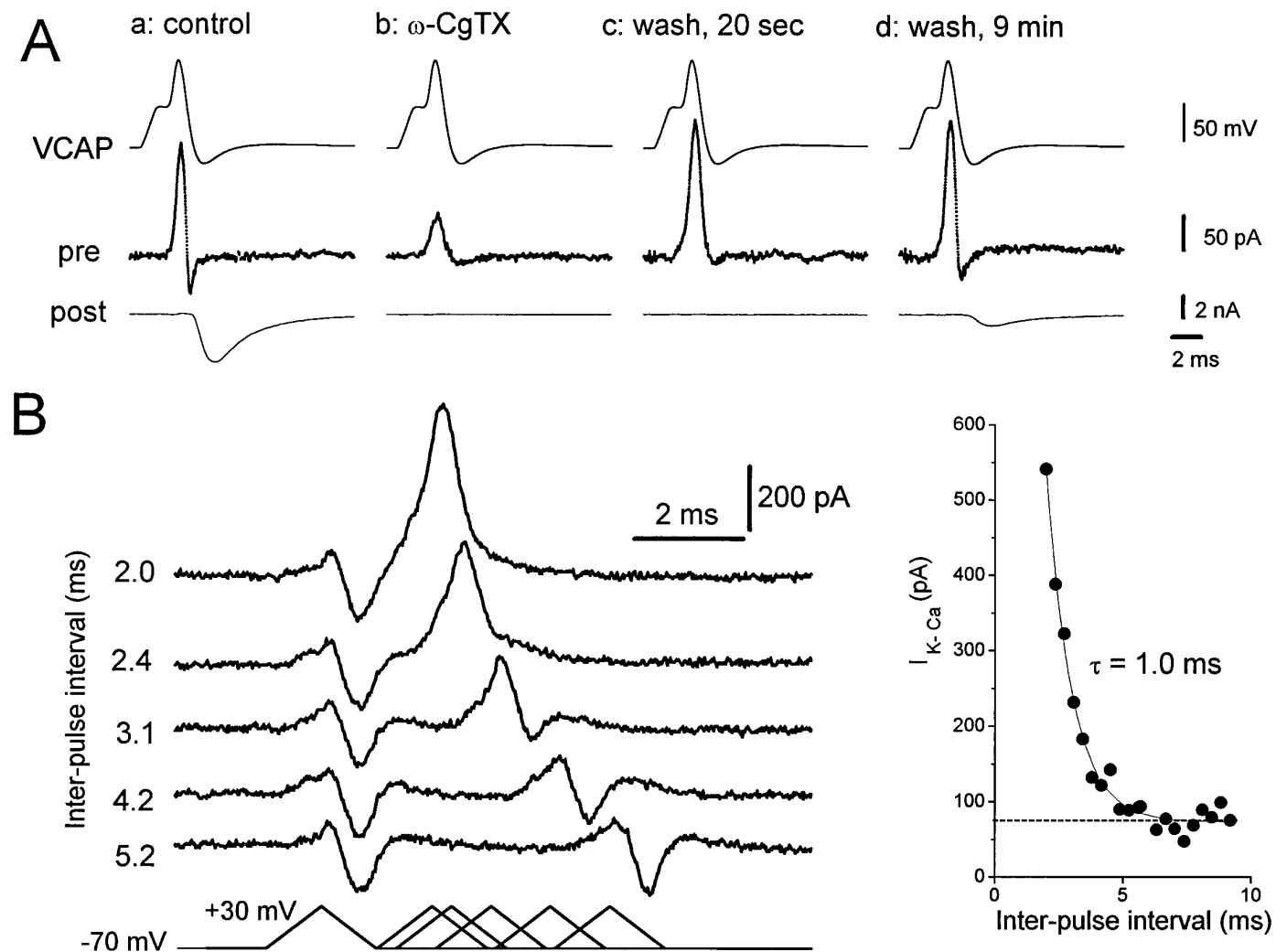
Figure 7. Evidence for coactivation of Ca and Ca-activated K currents. Experiments were performed with preparations treated with TTX and DAP. *A*, *a: control*, A VCAP waveform generated an early outward current, associated with the rising phase of the VCAP, and a smaller inward current (*pre*) correlated with transmitter release (*post*). *b: ω-CgTX*, 1 µM ω-CgTX reduced both presynaptic currents and eliminated the EPSC. *c: wash, 20 sec*, After a short washout of the toxin, most of the outward current recovered, but there was no detectable EPSC. *d: wash, 9 min*, After extensive washing, the inward Ca current and EPSC had recovered partially. The presynaptic electrode contained internal solution B. Similar results were seen at three other synapses. *B*, Activation of the Ca-activated K current by a ramp depolarization simulating an action potential. *Bottom, left*, Paired ramp depolarizations given to a presynaptic varicosity with varying interpulse interval from 2.0 msec (the second pulse given immediately after the end of the first pulse) to 5.2 msec. *Top, left*, The magnitude of the outward current in response to the second ramp was greatly increased at the minimum interpulse interval and decreased with increasing interpulse interval, approaching the magnitude of responses to the first ramp after ∼4 msec. The results were unchanged by reversing the order of ramp application (i.e., if the longest interpulse interval was applied first). *Right*, The outward current magnitude for the second ramp (ordinate) is plotted against the interpulse interval (abscissa). The outward current is predominantly Ca-activated K current, but its magnitude is an underestimate caused by the overlapping Ca current. The *solid line* is a single exponential regression line fitted to the data points ($\tau = 1.0$ msec), and the *dotted line* is the average outward current for the first ramp. Internal solution B was used. Similar results were seen in four other experiments.

involvement in neurotransmitter release, can be studied precisely under voltage control of the presynaptic varicosity.

Coupling of neurotransmitter release to I_{Ca} under steady-state voltage conditions

The quantitative correlation of presynaptic calcium entry with the amount of neurotransmitter release requires ideal conditions and possibly various methods of synaptic stimulation and analysis. In our preparation we were confident of these comparisons only for Ca currents generated by low-voltage stimulations. We are aware that analysis of data obtained with other protocols, for example using Ca tail currents or action potential waveforms, may yield

additional information. Nevertheless, our mean power-law relationship (1.76) is similar to that of Takahashi et al. (1996), who also used step waveforms and compared peak calcium tails with peak postsynaptic currents. On the other hand, values of 1–4 have been obtained at the squid giant synapse when presynaptic currents were compared with postsynaptic responses during step depolarizations at normal, constant extracellular Ca^{2+} concentrations (Llinás et al., 1981; Augustine and Charlton, 1986). In the classic paper on mature neuromuscular junctions, Dodge and Rahamimoff (1967) reported a value of 4 obtained with changes in external Ca^{2+} concentration. In a recent report of experiments on

the calyx of Held, Borst and Sakmann (1996), using action potential waveform depolarizations, found a fourth order relationship between peak Ca current and peak postsynaptic response. It is possible that these different numerical correlations between I_{Ca} and release can be explained by the different methods used. For example, longer depolarizations during step pulses allow more Ca^{2+} entry, which may partially saturate the Ca-acceptor molecule(s), reducing the cooperativity, as has been suggested by Stanley (1986).

The timing of Ca^{2+} entry during an action potential and coupling of neurotransmitter release to I_{Ca} in the action potential

The varicosity–muscle cell preparation has advantages over many other preparations in allowing isolation and direct measurement of each ionic current, including direct measurements of Ca^{2+} entry, during an action potential waveform. Currents can be correlated with release, synaptic delays can be measured under (relatively) physiological conditions, and release can be resolved at the quantal level.

We show that Ca^{2+} entry occurred primarily during the falling phase of the action potential (Fig. 6*C*). Similar results were obtained at squid synapses (Llinás et al., 1982), and comparable conclusions have been reached in studies of other, nonsynaptic preparations (McCobb and Beam, 1991; Scroggs and Fox, 1992; Wheeler et al., 1996) and recently in a CNS synapse (Borst and Sakmann, 1996). In addition, we detect a significant Ca^{2+} entry during the rising phase of the action potential (Fig. 6*C*), as has been reported recently at a mammalian synapse (Sabatini and Regehr, 1996). Although it is difficult to determine whether this early Ca^{2+} current is itself sufficient to evoke transmitter release, it probably participates in the activation of K_{Ca} channels.

Synaptic delay

The average synaptic delay of 630 µsec between the end of a step depolarization and the onset of transmitter release (Table 1*D*) identifies the cultured *Xenopus* neuromuscular junction as a fast synapse. Interestingly, this value was approximately the same as the "physiological" synaptic delay we measured between the time of maximal rate of rise of the I_{Ca} during the repolarization phase of the action potential and the onset of the EPSC (700 µsec) (Table 1*C*). The shortest delay we measured was 350 µsec, slightly longer than the 180 µsec minimum delay seen at the squid synapse (Llinás et al., 1981).

We observed similar synaptic delays between the maximum rate of rise of the action potential and the onset of the EPSC and between the maximum rate of rise of the voltage in a VCAP waveform and the EPSC (~1.3 and 1.5 msec) (see Table 1, columns A and B). This finding verifies the validity of using the VCAP waveform in experiments measuring presynaptic currents coupled to transmitter release. Moreover, these values were only slightly longer than the value (~1.1–1.2 msec) found at the mature neuromuscular junction by Katz and Miledi (1965). This similarity to the mature synaptic delay adds to the evidence that the varicosity synapses have well developed release machinery. Why both varicosity and mature neuromuscular junctions exhibit longer delays than does the squid synapse (minimum delay of 200 µsec) is not obvious. Ca^{2+} triggering and vesicle exocytosis are complicated processes, undoubtedly capable of adaptation to an increase or decrease in the speed of coupling, and the squid giant fiber system is a critical link in what has evolved to become a fast escape response.

Types of Ca channels and their coupling to transmitter release

In view of our finding that 1–2 µM ω-CgTX blocks all transmitter release in parallel with ~85% of the presynaptic Ca current, we conclude that transmitter release is dependent on Ca^{2+} entry through N-type Ca channels. This is consistent with findings at mature frog neuromuscular junctions, at which it has been shown that ω-CgTX blocks all evoked transmitter release (Kerr and Yoshikami, 1984; Koyano et al., 1987; Katz et al., 1995) and some spontaneous release (Grinnell and Pawson, 1989). In the present study, nimodipine blocked ~17% of I_{Ca}, suggesting the presence of L-type Ca channels as well. Although we did not test the effect of nimodipine on release, application of nimodipine and ω-CgTX had no greater blocking effect than ω-CgTX alone, suggesting that both agents may work on the same channels, for which there is some precedent (Jones and Jacobs, 1990; Wang et al., 1992; Reeve et al., 1994). The remaining ω-CgTX-insensitive current has not been identified but was not blocked by ω-AGA-IVA; therefore, it was apparently not P-type (Mintz et al., 1992). Finally, the residual current was incapable of evoking release and not merely insufficient in magnitude, because similarly small ω-CgTX-sensitive currents were capable of evoking release. Because our primary interest was in the Ca channels important for transmitter release, we have not yet made a more systematic study of the residual Ca current.

Coactivation of K_{Ca} channels with Ca channels during an action potential

Our results show that K_{Ca} channels are activated by Ca^{2+} entry during the rising phase of an action potential that initiates transmitter release (Fig. 7*A*). A close physical and functional association among K_{Ca} channels, Ca channels, and presynaptic release sites has been demonstrated at adult neuromuscular junctions (Cohen et al., 1991; Robitaille and Charlton, 1992; Robitaille et al., 1993) and in hair cells (Roberts et al., 1990). Because K_{Ca} channel activation and transmitter release occur in a small window of time (the action potential) in parallel with the Ca^{2+} entry, it is probable that this is true in the *Xenopus* varicosities as well.

It is desirable to know the channel densities and distributions in the varicosities. Assuming a Ca single channel conductance of 1.2 pS in normal extracellular Ca^{2+} (1.8 mM) (Church and Stanley, 1995), it can be estimated that the mean open Ca channel density obtained with step pulses was 2232 ± 1313 channels/varicosity, or 3.3 ± 2.2 channels/µm² (data presented in Fig. 3). For K_{Ca} channels, the mean number of open channels/varicosity was estimated to be 109 ± 53, or 0.10 ± 0.04/µm², assuming a single-channel conductance of 77 pS (Roberts et al., 1990). If one assumes, as has been demonstrated in other preparations (Roberts et al., 1990; Robitaille et al., 1993), that most of the K_{Ca} channels are located at the synaptic contact area where the Ca channels are concentrated, this would result in a calculated ratio of Ca channels to K_{Ca} channels of ~15–30. Furthermore, it is estimated on the basis of the data from Figures 6*C* and 7*A* that the opening of ~700 Ca channels and 15 K_{Ca} channels occurs in the presynaptic varicosity during the generation of EPSCs by action potentials.

K_{Ca} channels as Ca^{2+} sensors

In our preparation, K_{Ca} channels respond very quickly to Ca^{2+} entry during an action potential. Because of this behavior, the K_{Ca} channel activation can be used to estimate the persistence of Ca^{2+} in the submembranous space after an action potential. As is

shown in Figure 7*B*, the second of a pair of depolarizing ramps elicits a K_{Ca} current that is enhanced compared with the first. The decay time constant of enhancement was 1 msec (Fig. 7*B*, *right*). This might represent the closing time of K_{Ca} channels opened by Ca^{2+} entry in the first pulse. Alternatively, because the return of K_{Ca} current precedes the return of transmitter release after removal of block by ω-CgTX (Fig. 7*A*), K_{Ca} channels have an apparently higher effective sensitivity to Ca^{2+} than does the release mechanism. Given this higher sensitivity, the time constant of decay of potentiation of the K_{Ca} current in Figure 7*B* may represent a sensitive measure of the persistence of free Ca^{2+} near K_{Ca} channels. This decay may give an upper limit to the time within which the presynaptic Ca^{2+} concentrations fall below threshold for neurotransmitter release after an action potential.

Conclusions

The cultured *Xenopus* varicosity–muscle preparation allows the simultaneous study of pre- and postsynaptic currents at a synapse where release can be resolved at the single quantum level. We have shown that ω-CgTX GVIA-sensitive Ca currents (N-type) predominate and regulate neurotransmitter release at these varicosities but that other minority Ca currents also exist. Calcium entry occurs primarily during the falling phase of the presynaptic action potential, and the delay between Ca^{2+} entry and release in this preparation is 600–700 μsec. In addition, we have demonstrated that calcium-activated potassium channels are expressed in these transmitter-releasing varicosities and have provided biophysical evidence that they are coactivated with calcium channels at release sites. This preparation should prove useful for many future physiological, biophysical, biochemical, cellular, and molecular studies of synaptic function.

REFERENCES

Anderson MJ, Cohen MW, Zorychta E (1977) Effects of innervation on the distribution of acetylcholine receptors on cultured muscle cells. J Physiol (Lond) 268:731–756.

Artalejo CR, Adams ME, Fox AP (1994) Three types of Ca^{2+} channel trigger secretion with different efficacies in chromaffin cells. Nature 367:72–76.

Augustine GJ (1990) Regulation of transmitter release at the squid giant synapse by presynaptic delayed rectifier potassium current. J Physiol (Lond) 431:343–364.

Augustine GJ, Charlton MP (1986) Calcium dependence of presynaptic calcium current and post-synaptic response at the squid giant synapse. J Physiol (Lond) 381:619–640.

Augustine GJ, Eckert R (1982) Calcium-dependent potassium current in squid presynaptic nerve terminals. Biol Bull 163:397.

Augustine GJ, Charlton MP, Smith SJ (1985a) Calcium entry into voltage-clamped presynaptic terminals of squid. J Physiol (Lond) 367:143–162.

Augustine GJ, Charlton MP, Smith SJ (1985b) Calcium entry and transmitter release at voltage-clamped nerve terminals of squid. J Physiol (Lond) 367:163–181.

Augustine GJ, Charlton MP, Smith SJ (1987) Calcium action in synaptic transmitter release. Annu Rev Neurosci 10:633–693.

Barish ME (1991) Voltage-gated calcium currents in cultured embryonic *Xenopus* spinal neurones. J Physiol (Lond) 444:523–543.

Blatz AL, Magleby KL (1984) Ion conductance and selectivity of single calcium-activated potassium channels in cultured rat muscle. J Gen Physiol 84:1–23.

Blundon JA, Wright SN, Brodwick MS, Bittner GD (1995) Presynaptic calcium-activated potassium channels and calcium channels at a crayfish neuromuscular junction. J Neurophysiol 73:178–189.

Borst JGG, Sakmann B (1996) Calcium influx and transmitter release in a fast CNS synapse. Nature 383:431–434.

Borst JGG, Helmchen F, Sakmann B (1995) Pre- and postsynaptic whole-cell recordings in the medial nucleus of the trapezoid body of the rat. J Physiol (Lond) 489.3:825–840.

Brehm P, Kidokoro Y, Moody-Corbett F (1984) Acetylcholine receptor channel properties during development of *Xenopus* muscle cells in culture. J Physiol (Lond) 357:203–217.

Buchanan J, Sun YA, Poo M-M (1989) Studies of nerve–muscle interactions in *Xenopus* cell culture: fine structure of early functional contacts. J Neurosci 9:1540–1554.

Candia S, Garcia ML, Latorre R (1992) Mode of action of iberiotoxin, a potent blocker of the large conductance Ca^{2+}-activated K^+ channel. Biophys J 63:583–590.

Charlton MP, Smith SJ, Zucker RS (1982) Role of presynaptic calcium ions and channels in synaptic facilitation and depression at the squid giant synapse. J Physiol (Lond) 323:173–193.

Church PJ, Stanley EF (1995) Single calcium channel currents recorded at physiological calcium levels. Soc Neurosci Abstr 21 (Part 2):1578.

Cohen I, Van der Kloot W (1985) Calcium and transmitter release. Int Rev Neurobiol 27:299–336.

Cohen MW, Weldon PR (1980) Localization of acetylcholine receptors and synaptic ultrastructure at Nerve–Muscle contacts in culture: dependence on nerve type. J Cell Biol 86:388–401.

Cohen MW, Jones OT, Angelides KJ (1991) Distribution of Ca^{2+} channels on frog motor nerve terminals revealed by fluorescent ω-conotoxin. J Neurosci 11:1032–1039.

Dodge Jr FA, Rahamimoff R (1967) Co-operative action of calcium ions in transmitter release at the neuromuscular junction. J Physiol (Lond) 193:419–432.

Dunlap K, Luebke JI, Turner TJ (1994) Identification of calcium channels that control neurosecretion Science 266:828–831.

Evers J, Laser M, Sun YA, Xie ZP, Poo M-M (1989) Studies of Nerve–Muscle interactions in *Xenopus* cell culture: analysis of early synaptic currents. J Neurosci 9:1523–1539.

Fu WM, Huang FL (1994) L-type Ca^{2+} channel is involved in the regulation of spontaneous transmitter release at developing neuromuscular synapses. Neuroscience 58:131–140.

Grinnell AD, Pawson PA (1989) Dependence of spontaneous release at frog junctions on synaptic strength, external calcium and terminal length. J Physiol (Lond) 418:397–410.

Heidelberger R, Heinemann C, Neher E, Matthews G (1994) Calcium dependence of the rate of exocytosis in a synaptic terminal. Nature 371:513–515.

Hodgkin AL, Huxley AF (1952) A quantitative description of membrane current and its application to conduction and excitation in nerve. J Physiol (Lond) 117:500–544.

Horn R, Marty A (1988) Muscarinic activation of ionic currents measured by a new whole-cell recording method. J Gen Physiol 92:145–159.

Hulsizer SC, Meriney SD, Grinnell AD (1991) Calcium currents in presynaptic varicosities of embryonic motoneurons. Ann NY Acad Sci 635:424–428.

Jones SW, Jacobs LS (1990) Dihydropyridine actions on calcium currents of frog sympathetic neurons. J Neurosci 10:2261–2267.

Jones SW, Marks TN (1989) Calcium currents in bullfrog sympathetic neurons. I. Activation kinetics and pharmacology. J Gen Physiol 94:151–167.

Katz B (1969) The release of neural transmitter substances. Liverpool, UK: Liverpool UP.

Katz B, Miledi R (1965) The measurement of synaptic delay, and the time course of acetylcholine release at the neuromuscular junction. Proc R Soc Lond [Biol] 161:483–495.

Katz B, Miledi R (1967) A study of synaptic transmission in the absence of nerve impulses. J Physiol (Lond) 192:407–436.

Katz B, Miledi R (1970) Further study of the role of calcium in synaptic transmission. J Physiol (Lond) 207:789–801.

Katz B, Miledi R (1979) Estimates of quantal content during "chemical potentiation" of transmitter release. Proc R Soc Lond [Biol] 205:369–378.

Katz E, Ferro PA, Cherksey BD, Sugimori M, Llinás R, Uchitel OD (1995) Effects of Ca^{2+} channel blockers on transmitter release and presynaptic currents at the frog neuromuscular junction. J Physiol (Lond) 486:695–706.

Kerr LM, Yoshikami D (1984) A venom peptide with a novel presynaptic blocking action. Nature 308:282–284.

Kidokoro Y, Sand O (1989) Action potentials and sodium inward currents of developing neurons in *Xenopus* Nerve–Muscle cultures. Neurosci Res 6:191–208.

Kidokoro Y, Yeh E (1982) Initial synaptic transmission at the growth cone in *Xenopus* Nerve–Muscle cultures. Proc Nat Acad Sci USA 79:6727–6731.

Kidokoro Y, Anderson MJ, Gruener R (1980) Changes in synaptic potential properties during acetylcholine receptor accumulation and neurospecific interactions in *Xenopus* Nerve–Muscle cell culture. Dev Biol 78:464–483.

Koyano K, Abe T, Nishiuchi Y, Sakakibara S (1987) Effects of synthetic omega-conotoxin on synaptic transmission. Eur J Pharmacol 135:337–343.

Kullberg RW, Lentz TL, Cohen MW (1977) Development of the myotomal neuromuscular junction in *Xenopus laevis*: an electrophysiological and fine-structural study. Dev Biol 60:101–129.

Lancaster B, Nicoll RA (1987) Properties of two calcium-activated hyperpolarizations in rat hippocampal neurones. J Physiol (Lond) 389:187–203.

Lim NF, Nowycky MC, Bookman RJ (1990) Direct measurement of exocytosis and calcium currents in single vertebrate nerve terminals. Nature 344:449–451.

Lindgren CA, Moore JW (1989) Identification of ionic currents at presynaptic nerve endings of the lizard. J Physiol (Lond) 414:201–222.

Llinás R, Steinberg IZ, Walton K (1981) Relationship between presynaptic calcium current and postsynaptic potential in squid giant synapse. Biophys J 33:323–51.

Llinás R, Sugimori M, Simon SM (1982) Transmission by presynaptic spike-like depolarizations in the squid giant synapse. Proc Natl Acad Sci USA 79:2415–2419.

Luebke JI, Dunlap K, Turner TJ (1993) Multiple calcium channel types control glutamatergic synaptic transmission in the hippocampus. Neuron 11:895–902.

MacKinnon R, Miller C (1988) Mechanism of charybdotoxin block of the high-conductance, Ca^{2+}-activated K^+ channel. J Gen Physiol 91:335–349.

Marty A (1981) Ca-dependent K channels with large unitary conductance in chromaffin cell membranes. Nature 291:497–500.

McCobb DP, Beam KG (1991) Action potential waveform voltage-clamp commands reveal striking differences in calcium entry via low and high voltage-activated calcium channels. Neuron 7:119–127.

Meriney SD, Hulsizer SC, Grinnell AD (1991) Calcium currents in varicosities of motoneuron neurites ending on muscle cells in vitro. Biomed Res 12:53–55.

Miller C, Moczydlowski E, Latorre R, Phillips M (1985) Charybdotoxin, a protein inhibitor of single Ca^{2+}-activated K^+ channels from mammalian skeletal muscle. Nature 313:316–318.

Mintz IM, Venema VJ, Swiderek KM, Lee TD, Bean BP, Adams ME (1992) P-type calcium channels blocked by the spider toxin ω-Aga-IVA. Nature 355:827–829.

Mintz IM, Sabatini BL, Regehr WG (1995) Calcium control of transmitter release at a cerebellar synapse. Neuron 15:675–688.

Niewkoop PD, Faber J (1967) Normal table of *Xenopus laevis* (Daudin). Amsterdam: North-Holland.

Pfrieger FW, Veselovsky NS, Gottmann K, Lux HD (1992) Pharmacological characterization of calcium currents and synaptic transmission between thalamic neurons in vitro. J Neurosci 12:4347–4357.

Plummer MR, Logothetis DE, Hess P (1989) Elementary properties and pharmacological sensitivities of calcium channels in mammalian peripheral neurons. Neuron 2:1453–1463.

Rae J, Cooper K, Gates P, Watsky M (1991) Low access resistance perforated patch recordings using amphotericin B. J Neurosci Methods 37:15–26.

Reeve HL, Vaughan PF, Peers C (1994) Calcium channel currents in undifferentiated human neuroblastoma (SH-SY5Y) cells: actions and possible interactions of dihydropyridines and omega-conotoxin. Eur J Neurosci 6:943–952.

Regehr WG, Mintz IM (1994) Participation of multiple calcium channel types in transmission at single climbing fiber to Purkinje cell synapses. Neuron 12:605–613.

Roberts WM, Jacobs RA, Hudspeth AJ (1990) Colocalization of ion channels involved in frequency selectivity and synaptic transmission at presynaptic active zones of hair cells. J Neurosci 10:3664–3684.

Robitaille R, Charlton MP (1992) Presynaptic calcium signals and transmitter release are modulated by calcium-activated potassium channels. J Neurosci 12:297–305.

Robitaille R, Garcia ML, Kaczorowski GJ, Charlton MP (1993) Functional colocalization of calcium and calcium-gated potassium channels in control of transmitter release. Neuron 11:645–655.

Sabatini BL, Regehr WG (1996) Timing of neurotransmission at fast synapses in the mammalian brain. Nature 384:170–172.

Scroggs RS, Fox AP (1992) Multiple Ca^{2+} currents elicited by action potential waveforms in acutely isolated adult rat dorsal root ganglion neurons. J Neurosci 12:1789–1801.

Sivaramakrishnan S, Laurent G (1995) Pharmacological characterization of presynaptic calcium currents underlying glutamatergic transmission in the avian auditory brainstem. J Neurosci 15:6576–6585.

Spitzer NC, Lamborghini JE (1976) The development of the action potential mechanism of amphibian neurons isolated in culture. Proc Natl Acad Sci USA 73:1641–1645.

Stanley EF (1986) Decline in calcium cooperativity as the basis of facilitation at the squid giant synapse. J Neurosci 6:782–789.

Stanley EF (1993) Single calcium channels and acetylcholine release at a presynaptic nerve terminal. Neuron 11:1007–1010.

Stanley EF, Goping G (1991) Characterization of a calcium current in a vertebrate cholinergic presynaptic nerve terminal. J Neurosci 11:985–993.

Tabti N, Poo MM (1991) Culturing spinal neurons and muscle cells from *Xenopus* embryos. In: Culturing nerve cells (Banker G, Goslin K, eds). pp 137–153. Cambridge, MA: MIT.

Tabti N, Poo MM (1994) Study on the induction of spontaneous transmitter release at early Nerve–Muscle contacts in *Xenopus* cultures. Neurosci Lett 173:21–26.

Takahashi T, Nakajima Y, Hirosawa K, Nakajima S, Onodera K (1987) Structure and physiology of developing neuromuscular synapses in culture. J Neurosci 7:473–81.

Takahashi T, Forsythe IA, Tsujimoto T, Barnes-Davis M, Onodera K (1996) Presynaptic calcium current modulation by a metabotropic glutamate receptor. Science 274:594–597.

Wang X, Treistman SN, Lemos JR (1992) Two types of high-threshold calcium currents inhibited by omega-conotoxin in nerve terminals of rat neurohypophysis. J Physiol (Lond) 445:181–199.

Weldon PR, Cohen MW (1979) Development of synaptic ultrastructure at neuromuscular contacts in an amphibian cell culture system. J Neurocytol 8:239–259.

Wheeler DB, Randall A, Tsien RW (1996) Changes in action potential duration alter reliance of excitatory synaptic transmission on multiple types of Ca^{2+} channels in rat hippocampus. J Neurosci 16:2226–2237.

Yawo H, Chuhma N (1994) Omega-conotoxin-sensitive and -resistant transmitter release from the chick ciliary presynaptic terminal. J Physiol (Lond) 477:437–448.

Yawo H, Momiyama A (1993) Re-evaluation of calcium currents in pre- and postsynaptic neurones of the chick ciliary ganglion. J Physiol (Lond) 460:153–172.

Yazejian B, DiGregorio D, Grinnell AD, Vergara JL (1995) Calcium entry during the repolarization phase of the presynaptic action potential synchronizes the onset of post-synaptic currents. Biophys J 68:A347.